Anesthesiology 2007; 106:723–35

Regional Gas Exchange and Cellular Metabolic Activity in Ventilator-induced Lung Injury

Guido Musch, M.D., Jose G. Venegas, Ph.D.,† Giacomo Bellani, M.D.,‡ Tilo Winkler, Ph.D.,§ Tobias Schroeder, M.Eng.,‖ Bodil Petersen, M.D.,‖ R. Scott Harris, M.D.,# Marcos F. Vidal Melo, M.D., Ph.D.**

Background: **Alveolar overdistension and repetitive derecruitment–recruitment contribute to ventilator-induced lung injury (VILI). The authors investigated (1) whether inflammatory cell activation due to VILI was assessable by positron emission tomography and (2) whether cell activation due to dynamic overdistension alone was detectable when other manifestations of VILI were not yet evident.**

Methods: **The authors assessed cellular metabolic activity with [^{18}F]fluorodeoxyglucose and regional gas exchange with [^{13}N]nitrogen. In 12 sheep, the left ("test") lung was overdistended with end-inspiratory pressure of 50 cm H_2O for 90 min, while end-expiratory derecruitment of this lung was either promoted with end-expiratory pressure of −10 cm H_2O in 6 of these sheep (negative end-expiratory pressure [NEEP] group) or prevented with +10 cm H_2O in the other 6 (positive end-expiratory pressure [PEEP] group) to isolate the effect of overdistension. The right ("control") lung was protected from VILI.**

Results: **Aeration decreased and shunt fraction increased in the test lung of the NEEP group. [^{18}F]fluorodeoxyglucose uptake of this lung was higher than that of the control lung and of the test lung of the PEEP group, and correlated with neutrophil count. When normalized by tissue fraction to account for increased aeration of the test lung in the PEEP group, [^{18}F]fluorodeoxyglucose uptake was elevated also in this group, despite the fact that gas exchange had not yet deteriorated after 90 min of overdistension alone.**

Conclusion: **The authors could detect regional neutrophil activation in VILI even when end-expiratory derecruitment was prevented and impairment of gas exchange was not evident. Concomitant end-expiratory derecruitment converted this activation into profound inflammation with decreased aeration and regional shunting.**

This article is accompanied by an Editorial View. Please see: Simon BA: Imaging inflammation in acute lung injury. ANESTHESIOLOGY 2007; 106:656–8.

VENTILATOR-INDUCED lung injury (VILI) can contribute to the morbidity and mortality of patients with acute lung injury (ALI).[1] Overdistension, repetitive alveolar derecruitment and recruitment, and large tidal excursion are three physical determinants of VILI.[2–10] Because the pulmonary inflammatory process triggered by these physical stimuli is an important pathogenic event of VILI, a method to assess activation of inflammatory cells in the lung noninvasively and *in vivo* could be valuable, especially if it provided topographical information allowing identification of lung regions most affected by the inflammatory process of VILI.

Among the inflammatory cells involved in VILI, neutrophils have been shown to be sensitive to the pattern of mechanical ventilation.[11–13] Furthermore, neutrophil depletion attenuated,[14] whereas neutrophil stimulation worsened,[15] the pulmonary injury associated with mechanical ventilation. These observations point to a prominent role of neutrophils in VILI.[16] Metabolic activity of neutrophils can be assessed *in vivo* and noninvasively by imaging, with positron emission tomography (PET), the regional uptake of 2-[^{18}F]fluoro-2-deoxy-D-glucose ([^{18}F]FDG).[17–24] The topographic association between neutrophil activity and impairment of gas exchange can be investigated by imaging both [^{18}F]FDG and [^{13}N]nitrogen ($^{13}N_2$) infused intravenously in saline solution.

In this study, we used PET imaging of the pulmonary kinetics of [^{18}F]FDG and $^{13}N_2$ to measure regional metabolic activity of neutrophils and gas exchange in a sheep model of unilateral VILI. To induce unilateral VILI,[25] we used separate ventilation: The left ("test") lung was injuriously ventilated, while the right ("control") lung was protected from VILI. In one group of animals, the test lung was injured with both end-inspiratory overdistension and end-expiratory derecruitment to assess whether [^{18}F]FDG uptake was increased in a lung with VILI compared with an uninjured lung. In a second group, the test lung was also dynamically overdistended, but positive end-expiratory pressure (PEEP) was applied to prevent end-expiratory derecruitment and delay VILI induced by the same level of end-inspiratory pressure as in the first group.[26] In this second group, we assessed whether metabolic activation could be detected early during pure overdistension, when other manifestations of VILI, such as impairment of gas exchange, decreased respiratory compliance, and histopathologic changes,[2–4] had not yet occurred.

By imposing marked pressure changes on a uniform

* Assistant Professor of Anesthesia, † Associate Professor of Anesthesia, § Instructor in Anesthesia, ‖ Research Fellow, Department of Anesthesia and Critical Care, # Assistant Professor of Medicine, Pulmonary and Critical Care Unit, Department of Medicine, Massachusetts General Hospital and Harvard Medical School, Boston, Massachusetts. ‡ Research Fellow, Department of Experimental and Environmental Medicine and Biotechnology, Ospedale San Gerardo and Università Milano-Bicocca, Monza, Italy.

Received from the Department of Anesthesia and Critical Care, Massachusetts General Hospital and Harvard Medical School, Boston, Massachusetts. Submitted for publication August 25, 2006. Accepted for publication November 29, 2006. Supported by grant Nos. HL-076464, GM-007592, and HL-068011 from the National Institutes of Health, Bethesda, Maryland, and by a Research Training Grant awarded jointly from the Foundation for Anesthesia Education and Research, Rochester, Minnesota, and the American Society of Critical Care Anesthesiologists, Park Ridge, Illinois. Presented in part at the Annual Meeting of the American Society of Anesthesiologists, Las Vegas, Nevada, October 23, 2004.

Address correspondence to Dr. Musch: Department of Anesthesia and Critical Care, CLN 309, Massachusetts General Hospital, 55 Fruit Street, Boston, Massachusetts 02114. gmusch@partners.org.

healthy lung, we aimed at achieving controlled levels of mechanical stress that could be comparable to those that develop regionally in the heterogeneously inflated acutely injured lung.[27] Therefore, this experimental study aimed at assessing the direct contribution of mechanical stress associated with overdistension and repetitive derecruitment to inflammatory cell activation and regional gas exchange impairment, not at evaluating viable clinical ventilatory strategies or at reproducing multiple nonmechanical factors that can modulate VILI in patients with ALI, such as preexisting blood-borne injury to the lung,[28,29] surfactant dysfunction,[30] or infection.[31]

Materials and Methods

Experimental Preparation

The experimental procedures were approved by the Subcommittee on Research Animal Care of the Massachusetts General Hospital (Boston, Massachusetts). Twelve sheep, weighing 25.7 ± 2.9 kg (mean ± SD) (range, 20.5–30 kg) were fasted overnight and premedicated with intramuscular midazolam (2 mg/kg) and ketamine (4 mg/kg) in the morning. After intravenous induction of anesthesia with thiopental (30 mg/kg) and fentanyl (12.5–25 μg/kg), a cuffed endotracheal tube (HiLo Tube; Mallinckrodt Medical Inc., St. Louis, MO) was inserted through a tracheotomy. Anesthesia was maintained with a continuous infusion of thiopental (15–25 mg · kg^{-1} · h^{-1}) and fentanyl (10 - 30 μg · kg^{-1} · h^{-1}). After induction of anesthesia, paralysis was established with intravenous pancuronium (0.2 mg · kg^{-1} · h^{-1}), and the animals were ventilated in volume control mode with tidal volume of 11 ml/kg (end-inspiratory pressure, 16.2 ± 4.0 cm H_2O), respiratory rate of 18 breaths/min, inspiratory-to-expiratory time ratio of 1:1.5, and fraction of inspired oxygen of 1. Using aseptic surgical technique, an arterial and a Swan-Ganz catheter (model 831HF75; Edwards Lifesciences, Irvine, CA) were inserted through the femoral vessels, and a jugular venous catheter was placed for infusion of $^{13}N_2$ in saline solution and [^{18}F]FDG.

After surgical instrumentation of the animal was completed, the endotracheal tube was replaced with a 35-French left-sided double-lumen endobronchial tube to deliver injurious ventilation only to the left lung during the period of injury.[32,33] The double-lumen tube had been modified to accommodate sheep lung anatomy. The bronchial tip had been trimmed back approximately 3 mm to ensure ventilation of both left lobes, and the tracheal cuff had been moved 2 cm proximally to allow trimming of the distal tracheal opening of the double lumen tube and ensure adequate aeration of the right upper lobe. Proper position of the double lumen tube was confirmed by fiberoptic bronchoscopy. After airway instrumentation was completed, the animals were anticoagulated with intravenous heparin (200-U/kg bolus followed by an infusion at 50 U · kg^{-1} · h^{-1}) to prevent blood clotting in the intravascular catheters.

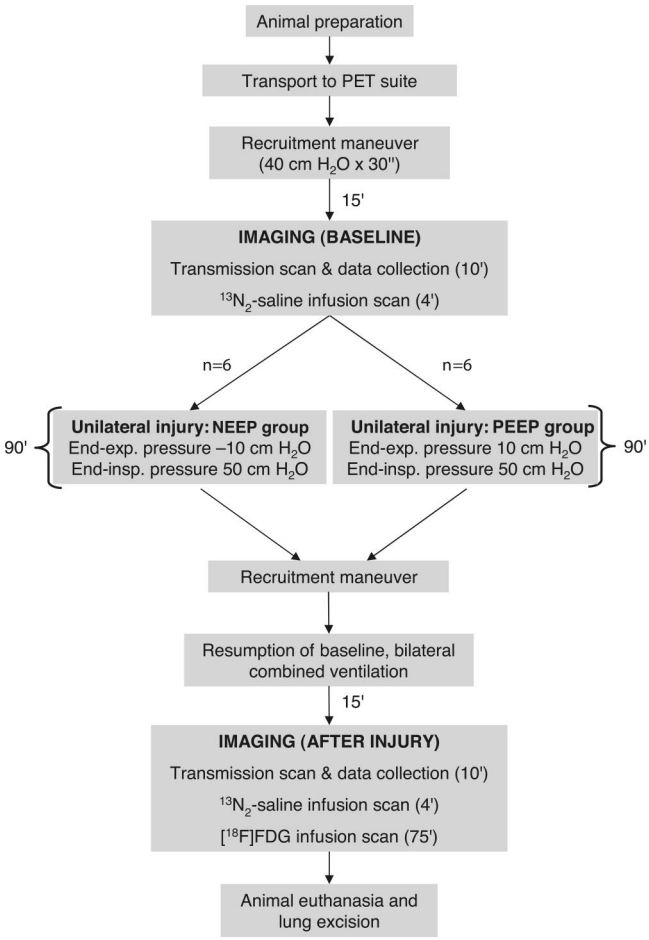

Fig. 1. Protocol schema. End-exp. = end-expiratory; End-insp. = end-inspiratory; [^{18}F]FDG = [^{18}F]fluorodeoxyglucose; n = sample size; $^{13}N_2$ = [^{13}N]nitrogen; NEEP = negative end-expiratory pressure; PEEP = positive end-expiratory pressure; PET = positron emission tomography.

The animals were then suspended prone in a cylindrical tube[34] and kept prone with unsupported abdomen for the remainder of the experiment. The rationale for the use of the suspended prone position was to favor homogeneous lung expansion and minimize baseline intraregional mechanical heterogeneity so that the whole lung could be regarded as an approximately uniform region.

Experimental Protocol

The protocol schema is shown in figure 1. After transport from the surgical preparation suite to the PET suite, the animals were placed prone in the PET scanner with the caudal end of the field of view just superior to the dome of the diaphragm. During transport (approximately 2 min), bilateral ventilation was provided with an Ambu bag. In the PET suite, the animals were connected to the mechanical ventilator used for $^{13}N_2$ scanning[35,36]

and, after a recruitment maneuver (airway pressure of 40 cm H_2O for 30 s), combined bilateral mechanical ventilation with baseline settings was resumed. Starting at 15 min after the recruitment maneuver, a 10-min PET transmission scan was acquired to measure regional aeration, and a complete set of baseline physiologic data was collected during the last 2 min of the transmission scan. After the transmission scan, a 4-min $^{13}N_2$–saline bolus infusion scan was acquired to measure regional perfusion and shunt. When baseline scans were completed, the animals were assigned to one of two groups of unilateral injurious ventilation. In both groups, injurious ventilation was delivered for 90 min only to the left (test) lung, while the right (control) lung was maintained at continuous positive airway pressure of 10 cm H_2O with a bias flow of 100% oxygen. Injurious ventilation was performed with a volume-cycled ventilator that delivered a half-sinusoidal inspiratory flow waveform (Harvard Apparatus, Millis, MA). Accordingly, during injury, end-inspiratory flow in the test lung approached zero and end-inspiratory airway pressure approximated plateau pressure. In both groups, tidal volume to the test lung was set to achieve end-inspiratory airway pressure of 50 cm H_2O. In one group (n = 6), negative end-expiratory pressure (NEEP) of −10 cm H_2O was applied to the test lung to promote end-expiratory alveolar derecruitment,[30,37] whereas in the other group (n = 6), PEEP of 10 cm H_2O was used to prevent derecruitment. NEEP was obtained by connecting the expiratory port of the Harvard ventilator to a Y tube that was open to atmosphere through an adjustable resistor on one arm and was connected to a vacuum source through the other arm. PEEP was obtained by connecting the expiratory port of the Harvard ventilator to a positive pressure valve. Respiratory rate of the test lung was set at 22 breaths/min, inspiratory-to-expiratory time ratio was set at 1:1, and fraction of inspired oxygen was left at 1. To prevent a possible injurious effect of hypocapnia from hyperventilation in the NEEP group,[38] an adjustable dead space volume was inserted proximally to the left bronchial port of the double-lumen tube, and respiratory rate could be varied by up to 2 breaths/min to keep arterial carbon dioxide tension ($Paco_2$) at or above 30 mmHg (arterial blood gases were measured intermittently throughout the period of injurious ventilation).

After 90 min of unilateral injurious ventilation, the Harvard ventilator was substituted with the ventilator system suitable for $^{13}N_2$ PET scanning and, after a recruitment maneuver, bilateral combined mechanical ventilation was resumed at baseline settings. Fifteen minutes later, transmission and $^{13}N_2$ PET scans were acquired, and a complete set of physiologic data was collected. After completion of the postinjury $^{13}N_2$ scan and clearance of $^{13}N_2$ radioactivity, [^{18}F]FDG was infused to measure metabolic activity.

At the end of the protocol, the animals were given additional anesthetics (30 mg/kg thiopental and 25 μg/kg fentanyl) and killed by intravenous potassium (40 mmol).

Table 1. Physiologic Variables during Unilateral Injurious Ventilation

	NEEP Group	PEEP Group
RR (test lung), breaths/min	21.8 ± 2.6	21.8 ± 2.3
TV (test lung), l	0.49 ± 0.15	0.27 ± 0.11*
$Flow_{mean\text{-}inspiratory}$ (test lung), l/s	0.38 ± 0.14	0.20 ± 0.07*
$Paw_{end\text{-}inspiratory}$ (test lung), cm H_2O	53.8 ± 3.7	52.3 ± 6.3
$Paw_{end\text{-}expiratory}$ (test lung), cm H_2O	−10.8 ± 1.6	10.2 ± 0.4†
Paw_{mean} (test lung), cm H_2O	10.2 ± 6.2	20.7 ± 1.6†
$Paw_{continuous\text{-}positive}$ (control lung), cm H_2O	10.0 ± 1.4	10.8 ± 3.7
$Paco_2$, mmHg	44 ± 10	57 ± 9*
pHa	7.40 ± 0.12	7.36 ± 0.03
Pao_2, mmHg	336 ± 261	382 ± 133
BEa, mM	−1 ± 5	5 ± 2*
CO, l/min	2.6 ± 0.9	2.8 ± 0.8
HR, beats/min	105 ± 21	112 ± 32
MAP, mmHg	101 ± 16	104 ± 18
MPAP, mmHg	19 ± 5	19 ± 4

Data are presented as mean ± SD.

Negative end-expiratory pressure (NEEP) *vs.* positive end-expiratory pressure (PEEP) group (Mann–Whitney U test): * $P < 0.05$, † $P < 0.01$.

BEa = arterial base excess; CO = cardiac output; HR = heart rate; MAP = mean arterial pressure; MPAP = mean pulmonary arterial pressure; $Paco_2$ = arterial carbon dioxide tension; Pao_2 = arterial oxygen tension; Paw = pressure at the airway opening, measured separately in the injuriously ventilated (test) lung and in the control lung; pHa = arterial pH; RR = respiratory rate; TV = tidal volume.

Physiologic Data

Airway and systemic and pulmonary arterial pressures were measured using a strip chart recorder (Hewlett Packard Inc., Palo Alto, CA). During the period of unilateral injurious ventilation, pressure at the airway opening was measured separately in the test and control lungs to ensure adequate lung separation and maintenance of the set ventilatory parameters. Cardiac output was measured by thermodilution (model COM-1; Edwards Laboratory, Santa Ana, CA). Blood gases were measured using a blood gas analyzer (model ABL5/BPH5; Radiometer Medical, Copenhagen, Denmark). Oxygen saturation was estimated from the oxyhemoglobin dissociation curve for hemoglobin B in sheep.[39] Global shunt fraction was calculated from blood oxygen content with the Berggren equation.[40] Tidal volume was measured by integration of the flow signal. Before and after injury, quasi-static respiratory chord compliance was calculated with a 0.5-s end-inspiratory pause, according to standard formulas.[41]

For physiologic variables that were measured during injury, values recorded halfway through the period of unilateral injurious ventilation are reported (table 1). A complete set of physiologic data was collected before and after injury, when the animals were ventilated with bilateral combined mechanical ventilation (table 2).

Table 2. Global Physiologic Variables before and after Injury

	Baseline (NEEP Group)	Baseline (PEEP Group)	After Injury (NEEP Group)	After Injury (PEEP Group)
Crs, ml/cm H_2O	19.6 ± 5.3	23.0 ± 5.5	13.6 ± 3.8	22.4 ± 5.9‡
$Paco_2$, mmHg	39 ± 6	35 ± 2	40 ± 6	37 ± 4
pHa	7.47 ± 0.03	7.54 ± 0.04	7.43 ± 0.04	7.54 ± 0.03†
Pao_2, mmHg	516 ± 107	513 ± 72	438 ± 143	505 ± 86
BEa, mM	3 ± 2	7 ± 3	1 ± 2	8 ± 3*
$Pvco_2$, mmHg	45 ± 4	42 ± 3	48 ± 5	46 ± 4
pHv	7.42 ± 0.02	7.48 ± 0.03	7.38 ± 0.04	7.47 ± 0.02†
Pvo_2, mmHg	73 ± 23	52 ± 11	68 ± 12	53 ± 8
BEv, mM	4 ± 2	7 ± 2	3 ± 2	8 ± 2
Fso_2	0.10 ± 0.06	0.09 ± 0.06	0.15 ± 0.09	0.09 ± 0.06
CO, l/min	3.5 ± 1.2	3.1 ± 1.0	3.0 ± 0.9	3.0 ± 0.6
HR, beats/min	138 ± 40	131 ± 22	108 ± 38	113 ± 31‡
MAP, mmHg	113 ± 28	123 ± 12	97 ± 18	110 ± 11
MPAP, mmHg	14 ± 3	12 ± 4	17 ± 4	13 ± 4
PCWP, mmHg	5 ± 3	4 ± 2	6 ± 4	6 ± 4
T, °C	37.4 ± 2.1	38.0 ± 1.0	36.7 ± 2.6	37.2 ± 1.4

Data are presented as mean ± SD.

Negative end-expiratory pressure (NEEP) *vs.* positive end-expiratory pressure (PEEP) group, at baseline (Mann–Whitney U test): * $P < 0.05$, † $P < 0.01$; baseline *vs.* after injury, within group (Wilcoxon rank sign test): ‡ $P < 0.05$ (NEEP group).

BEa = arterial base excess; BEv = venous base excess; CO = cardiac output; Crs = respiratory system compliance; Fso_2 = global shunt fraction (Berggren equation); HR = heart rate; MAP = mean arterial pressure; MPAP = mean pulmonary arterial pressure; $Paco_2$= arterial carbon dioxide tension; Pao_2 = arterial oxygen tension; PCWP = pulmonary capillary wedge pressure; pHa = arterial pH; pHv = mixed venous pH; $Pvco_2$ = mixed venous carbon dioxide tension; Pvo_2 = mixed venous oxygen tension; T = body temperature.

Positron Emission Tomography Imaging

A PET scanner that imaged 15 contiguous, 6.5-mm-thick slices of thorax at a spatial resolution of 6-mm full width at half maximum was used (PC-4096; Scanditronix AB, Uppsala, Sweden). We previously estimated, in sheep of similar weight, that this field of view encompassed approximately 70% of the lung.[42] Emission scans were reconstructed with a filtered back projection algorithm and low-pass filtered to an effective in-plane spatial resolution of 13 × 13 mm. Therefore, the size of the final resolution element was 13 × 13 × 6.5 mm. Three types of PET scans were acquired:

Transmission (Density) Scan. Ten-minute transmission scans were acquired at baseline, halfway through the period of unilateral injury, and after injury. They were used to demarcate the lung field (see below) and to calculate gas fraction from the linear relation between tissue attenuation and lung density.[43,44] Gas fraction was measured for each voxel of lung. The fraction of the voxel's volume occupied by parenchyma, blood, inflammatory infiltrate, or edema was calculated as

$$\text{“Tissue” Fraction} = 1 - \text{Gas Fraction}.$$

Because the transmission scan cannot differentiate tissue components with similar density, tissue fraction, in the lung, represents the fractional content of all components with unit density and therefore includes not only the contribution of parenchyma but also of blood, inflammatory infiltrate, and edema.

Gas fraction of each lung was computed by averaging the corresponding voxel values. Lung volume was calculated as the product of the number of voxels within each lung field by the voxel's volume.

$^{13}N_2$–Saline Bolus Infusion (Perfusion) Scan. $^{13}N_2$ (19 ± 6 mCi) dissolved in saline solution (38 ± 2 ml) was infused through the jugular catheter as a bolus over the initial 3 s of a 60-s apnea. Apnea was performed at an airway pressure corresponding to the mean airway pressure measured during the preceding period of bilateral combined ventilation.[36] Simultaneously with the start of the $^{13}N_2$–saline infusion, the acquisition of a series of sequential PET frames (8 × 2.5 s, 10 × 10 s, 4 × 30 s) was initiated to measure the pulmonary kinetics of $^{13}N_2$. Because of the low solubility of nitrogen in blood and tissues (partition coefficient water-to-air is 0.015 at 37°C), the pulmonary kinetics of infused $^{13}N_2$ (fig. 2) differ between regions that are perfused and aerated and regions containing alveolar units which, being perfused but not aerated, do not exchange gas (*i.e.*, shunting units). In perfused and aerated regions, virtually all $^{13}N_2$ diffuses into the alveolar airspace at first pass, where it accumulates in proportion to regional perfusion for the remainder of the apnea.[43,45] In regions that contain shunting alveolar units, $^{13}N_2$ kinetics during apnea show a peak of tracer concentration in the early PET frames, corresponding to arrival of the bolus of tracer with pulmonary blood flow, followed by an exponential decrease toward a plateau. This decrease of activity reflects lack of retention of $^{13}N_2$ in nonaerated units, and its magnitude is therefore related to regional shunt.[36,42] Perfusion and shunt fraction of the test and control lungs were calculated with a tracer kinetics model.[46,47]

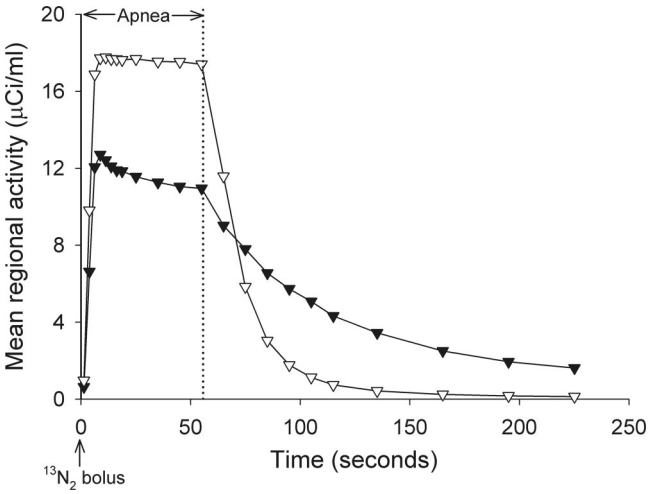

Fig. 2. Tracer kinetics of infused [^{13}N]nitrogen ($^{13}N_2$) after unilateral ventilator-induced lung injury to the test lung of one animal of the negative end-expiratory pressure group. After a 3-s intravenous injection of a bolus of $^{13}N_2$ dissolved in saline solution (*arrow*), positron emission tomography frames were acquired during 60 s of apnea (*left of vertical dotted line*) and 3 min of ensuing ventilation (*right of vertical dotted line*). $^{13}N_2$ kinetics during apnea in the test lung (*filled symbols*) show an early peak in tracer activity, corresponding to arrival of the bolus of tracer with pulmonary blood flow, followed by an exponential decrease toward a plateau. This decrease of activity is consistent with the presence of shunting alveolar units, which do not retain $^{13}N_2$ during apnea. In contrast, after rising with arrival of the bolus of tracer at the beginning of apnea, activity remains virtually constant in the control lung (*open symbols*), indicating normal gas exchange.

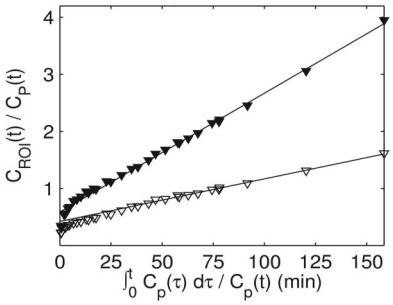

Fig. 3. Patlak plot: [^{18}F]fluorodeoxyglucose activity in a region of interest (C_{ROI}) of the test lung (*filled symbols*) and of the control lung (*open symbols*) normalized to plasma activity (C_P) *versus* the integral of plasma activity normalized to plasma activity, for one animal of the negative end-expiratory pressure group. After unilateral ventilator-induced lung injury to the test lung, [^{18}F]fluorodeoxyglucose uptake rate, calculated as the slope of the linear portion of the plot, is higher in the test than in the control lung.

Perfusion was normalized to tissue volume of each lung, measured from the corresponding transmission scan and defined as

$$\text{Tissue Volume} = \text{Tissue Fraction} \cdot \text{Lung Volume}.$$

Normalized perfusion was expressed in ml blood · min^{-1} · ml tissue^{-1}.

[^{18}F]FDG (Metabolic Activity) Scan. After $^{13}N_2$ clearance, [^{18}F]FDG (5–10 mCi) was infused through the jugular catheter over 60 s and, starting at the beginning of [^{18}F]FDG infusion, sequential PET frames (6 × 30 s, 7 × 60 s, 15 × 120 s, 1 × 300 s, 3 × 600 s) were acquired over 75 min while pulmonary arterial blood was sampled at the following intervals: 15 s × 3 min, 30 s × 2 min, 60 s × 5 min, 300 s × 55 min, followed by a last sample at 75 min. Blood samples (1 ml) were spun down, and the activity of plasma was measured in a gamma counter cross-calibrated with the PET scanner. [^{18}F]FDG PET scans were acquired only after injury because of the 110-min half-life of [^{18}F]fluoride.

After being transported into the cell by the same mechanism as glucose, [^{18}F]FDG is phosphorylated by hexokinase to [^{18}F]FDG-6-phosphate, which accumulates in proportion to the metabolic rate of the cell. [^{18}F]FDG net uptake rate, a measure of cellular metabolic activity, was calculated with the graphical method of Patlak *et al.*[48,49] by plotting lung activity normalized to plasma activity *versus* the integral of plasma activity normalized to plasma activity. At steady state of tracer transfer between plasma and intracellular compartments, the plot becomes a straight line (in the lung, usually 8–10 min after injection of [^{18}F]FDG), the slope of which corresponds to the [^{18}F]FDG uptake rate (fig. 3). [^{18}F]FDG uptake rate was calculated for each voxel in the lung field and displayed as a parametric image of metabolic activity (fig. 4). To account for the effect of variations in lung density on local [^{18}F]FDG uptake, we normalized the uptake rate by tissue fraction and defined specific metabolic activity (*i.e.*, [^{18}F]FDG uptake rate per unit of tissue) as

$$[^{18}\text{F}]\text{FDG Uptake Rate} \cdot (\text{Tissue Fraction})^{-1}.$$

The normalized rate is expected to account for differences in lung inflation or volume of inflammatory infiltrate and exudate.[19] [^{18}F]FDG uptake of each lung was obtained by averaging the corresponding voxel values.

To ascertain the contribution of neutrophils to the [^{18}F]FDG signal, two additional sheep were submitted to the NEEP injury protocol after either moderate (4-day treatment) or severe (8-day treatment) systemic neutrophil depletion with intravenous hydroxyurea (200 mg · kg^{-1} · day^{-1}). In these two sheep, and in the sheep studied last in the NEEP group, blood neutrophils were counted on the day of the experiment to investigate the relation between [^{18}F]FDG uptake rate and *circulating* neutrophil count.

To assess the effect of NEEP *per se* (*i.e.*, in the absence of end-inspiratory overdistension and large tidal volume) on [^{18}F]FDG uptake, two sheep underwent 90 min of separate ventilation with the test lung ventilated at NEEP of –10 cm H_2O, end-inspiratory pressure of 15 cm H_2O (tidal volume, 6.0 and 6.6 ml/kg), respiratory rate of 22 breaths/min, and inspiratory-to-expiratory time ratio of 1:1. To prevent hypercapnia, the control lung was also ventilated in these two sheep, with end-inspiratory pres-

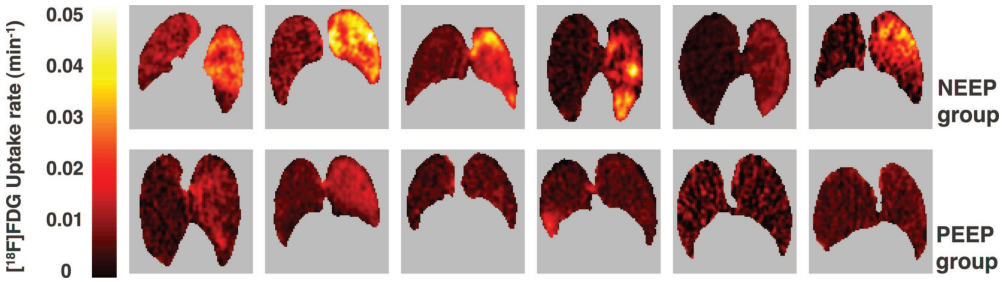

Fig. 4. Parametric images of [^{18}F]fluorodeoxyglucose ([^{18}F]FDG) uptake rate after unilateral ventilator-induced lung injury to the test lung of animals in the negative end-expiratory pressure (NEEP) group (*upper row*) and in the positive end-expiratory pressure (PEEP) group (*lower row*). Looking at each image, the test lung is on the *right*, and the control lung is on the *left*. One slice is shown for each animal.

sure of 15 cm H_2O (tidal volume, 4.4 and 3.8 ml/kg), respiratory rate of 15 breaths/min, inspiratory-to-expiratory time ratio of 1:1.5, and no PEEP. With these settings, $Paco_2$ was 31 and 35 mmHg in the two animals halfway through the period of separate ventilation. Fraction of inspired oxygen was left at 1.

Demarcation of the Lung Field. Aerated lung regions were identified by applying a threshold to the transmission scan.[43,44] Perfused regions were identified by applying a threshold to the early frames of the $^{13}N_2$–saline bolus infusion scan.[34,36] A lung field mask was created, for each lung of each animal, from the union of aerated regions and of perfused regions, and was refined by hand to exclude main bronchi and large pulmonary vessels.

Histologic Analysis

At the end of the study protocol, lung histologic analysis was performed in all animals of the PEEP group and in three animals of the NEEP group. The lungs were excised and suspended, and the trachea was connected to a reservoir containing Trump fixative (4% formaldehyde and 1% glutaraldehyde in phosphate-buffered saline). The lungs were filled with fixative to a pressure of 25 cm H_2O, the trachea was clamped, and the lungs were submersed in a container filled with fixative and stored for 7 days at 4°C. After fixing, the lungs were cut in 1-cm-thick slices along the sagittal plane, and the second most lateral slice of each lung was selected for further histologic analysis (the most lateral slice was fully covered with pleura on its lateral aspect, which would have made it harder for the embedding resin to penetrate, whereas more medial slices contained large vessels and airways). Using a stratified random sampling technique, a 1-cm^3 block of lung tissue was selected from each of the ventral, middle, and dorsal regions of the slice. The tissue block was embedded in Technovit 7100 resin (Heraeus Kulzer, Wehrheim, Germany), and 2-μm-thick sections were cut, mounted, and stained with 0.01% toluidine blue for light microscopy.[50] Extravascular lung neutrophils were counted in 240 randomly selected high-power (40×) fields (0.033 mm^2/field) per lung by a pathologist-trained physician who was blinded to the group assignment and to whether the lung was a test or a control lung.

Statistical Analysis

Statistical analysis was performed with nonparametric statistical tests (SPSS 13.0; SPSS Inc., Chicago, IL) to reduce the effect of single data values on small sample statistics. Differences within group, either between before and after injury or between the test and control lungs, were tested with Wilcoxon signed ranks test for matched pairs, because measurements were performed on the same animal. Differences between the two groups were tested with Mann–Whitney U test. Associations between variables were measured both with Pearson (parametric) correlation coefficient and with Spearman (nonparametric) rank coefficient.

For global physiologic variables (table 2), groups were compared at baseline, and the effect of injury was assessed within group by testing the difference between before and after injury. For PET-derived regional variables (figs. 5–7), differences between lungs were tested separately at baseline and after injury, because [^{18}F]FDG uptake could be measured only after injury (fig. 8).

Statistical significance was set at $P < 0.05$. Data are mean ± SD.

Results

Physiologic Variables during Unilateral Injurious Ventilation

As expected from the experimental protocol, tidal volume and mean inspiratory flow of the test (*i.e.*, injuriously ventilated) lung were higher in the NEEP than in the PEEP group (table 1). End-inspiratory airway pressure was similar in the test lung of the two groups. End-expiratory and mean airway pressures of the test lung were lower in the NEEP than in the PEEP group. The control lung was held at 10 cm H_2O of continuous positive airway pressure in both groups.

Consistent with the airway pressure data, the trans-

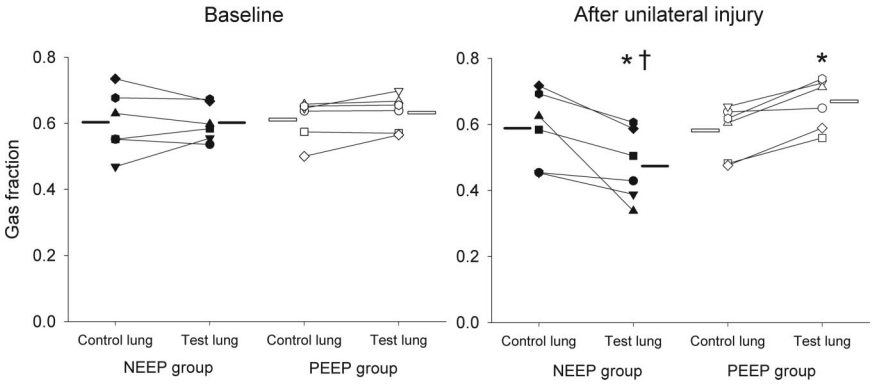

Fig. 5. Gas fraction before and after unilateral ventilator-induced lung injury to the test lung of animals in the negative end-expiratory pressure (NEEP) group (*filled symbols*) and in the positive end-expiratory pressure (PEEP) group (*open symbols*). *Horizontal dashes* indicate means. * $P < 0.05$ test *versus* control lung, within group. † $P < 0.05$ test lung of the NEEP group *versus* test lung of the PEEP group.

mission scan acquired halfway through the period of unilateral injurious ventilation showed a lower gas fraction in the test lung of the NEEP group than in that of the PEEP group (0.59 ± 0.07 *vs.* 0.83 ± 0.10; $P <$ 0.05) and no significant difference in gas fraction of the control lungs (0.66 ± 0.08 and 0.70 ± 0.15, respectively).

During the period of unilateral injurious ventilation, $Paco_2$ was higher in the PEEP than in the NEEP group, but pH was not significantly different between groups, probably because base excess was higher in the PEEP group. Arterial oxygen tension (Pao_2) and hemodynamics were not significantly different between groups (table 1).

Changes in Global Physiologic Variables between before and after Injury

At baseline, global physiologic variables were not significantly different between groups except pH and arterial base excess, which were higher in the PEEP group (table 2). $Paco_2$ tended to be lower, although not significantly, in the PEEP than in the NEEP group despite similar tidal volume (11.0 ± 0.6 and 10.7 ± 1.2 ml/kg, respectively) and respiratory rate (18.0 ± 0.4 and 17.7 ± 1.9 breaths/min). Respiratory system compliance, global shunt fraction, hemodynamics, and body temperature were not significantly different between groups at baseline.

Physiologic measurements performed after the end of unilateral injurious ventilation and resumption of bilateral combined ventilation at baseline settings showed that compliance had decreased with injury only in the NEEP group (table 2). In this group, Pao_2 tended to decrease and global shunt fraction tended to increase after injury, but these changes did not reach statistical significance. In the PEEP group, neither global gas exchange nor compliance was affected by the 90-min period of unilateral overdistension. Except for a decrease of heart rate in the NEEP group, changes in hemodynamics were not significant in either group.

Regional Aeration, Shunt Fraction, and Perfusion at Baseline and after Injury

Before injury, gas fraction (fig. 5), shunt fraction (fig. 6), and perfusion (fig. 7) were similar in the test and control lungs of both groups.

After the period of unilateral injurious ventilation, gas fraction of the test lung in the NEEP group became lower than that of the control lung (fig. 5). In the PEEP group, gas fraction of the test lung became higher than that of its control lung and of the test lung of the NEEP group. In the NEEP group, shunt fraction of the test lung became higher than that of the control lung (fig. 6), and the difference in shunt fraction between the test and control lungs (*i.e.*, the increase in regional shunt fraction attributable to localized VILI) was significantly greater than the increase in global shunt fraction (0.22 ± 0.17 *vs.* 0.05 ± 0.10; $P < 0.05$). In the PEEP group, shunt fraction remained similarly low in the test and control lungs. Accordingly, shunt fraction of the test lung became

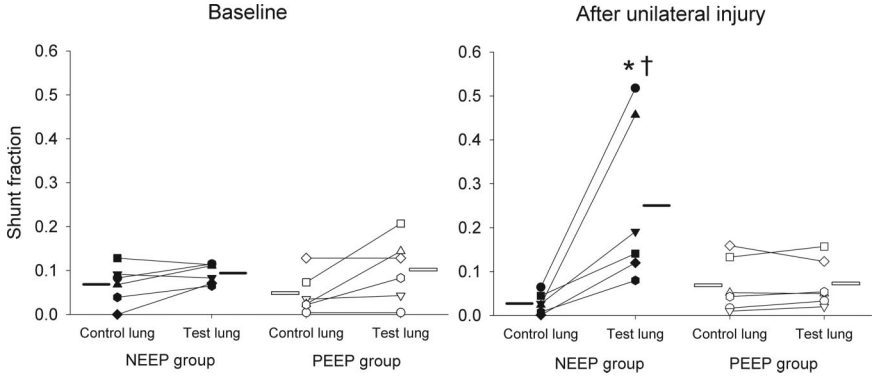

Fig. 6. Shunt fraction before and after unilateral ventilator-induced lung injury to the test lung of animals in the negative end-expiratory pressure (NEEP) group (*filled symbols*) and in the positive end-expiratory pressure (PEEP) group (*open symbols*). *Horizontal dashes* indicate means. * $P < 0.05$ test *versus* control lung, within group. † $P < 0.05$ test lung of the NEEP group *versus* test lung of the PEEP group.

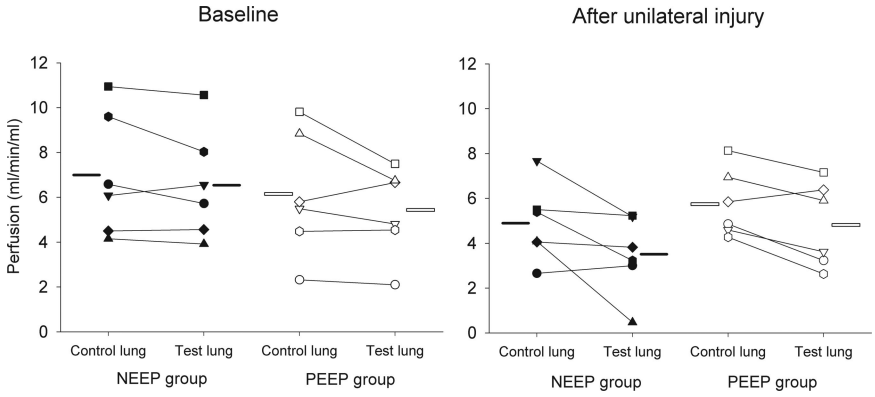

Fig. 7. Perfusion before and after unilateral ventilator-induced lung injury to the test lung of animals in the negative end-expiratory pressure (NEEP) group (*filled symbols*) and in the positive end-expiratory pressure (PEEP) group (*open symbols*). *Horizontal dashes* indicate means.

higher in the NEEP than in the PEEP group. Normalized perfusion was not significantly different between the test and control lungs, although five of six animals in both groups showed lower perfusion to the test than to the control lung after injury (fig. 7).

Regional Metabolic Activity

After unilateral injury, the [^{18}F]FDG uptake rate of the test lung in the NEEP group was higher than that of its control lung and of the test lung in the PEEP group (fig. 8A). The [^{18}F]FDG uptake rate was similar, on average, in the test and control lungs of the PEEP group, with three animals in this group showing higher [^{18}F]FDG uptake in the test than in the control lung and three animals showing higher uptake in the control lung. Interestingly, this inconsistent behavior among animals of the PEEP group was no longer present when local [^{18}F]FDG uptake rate was normalized by tissue fraction, as normalized [^{18}F]FDG uptake rate was higher in the test than in the control lung of all animals in the PEEP group (fig. 8B). Uptake of [^{18}F]FDG remained higher in the test than in the control lung of the NEEP group also after normalization. Uptake of [^{18}F]FDG was remarkably similar in the control lungs of the two groups.

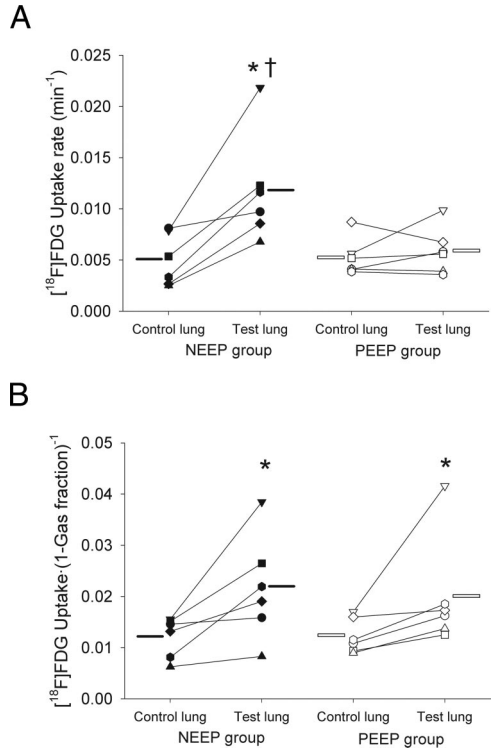

Fig. 8. (*A*) [^{18}F]fluorodeoxyglucose ([^{18}F]FDG) uptake rate after unilateral ventilator-induced lung injury to the test lung of animals in the negative end-expiratory pressure (NEEP) group (*filled symbols*) and in the positive end-expiratory pressure (PEEP) group (*open symbols*). *Horizontal dashes* indicate means. * $P < 0.05$ test *versus* control lung, within group. † $P < 0.05$ test lung of the NEEP group *versus* test lung of the PEEP group. (*B*) [^{18}F]FDG uptake rate normalized to tissue fraction (*i.e.*, specific metabolic activity).

In the two additional animals in which the test lung was ventilated at NEEP of −10 cm H_2O without end-inspiratory overdistension, the [^{18}F]FDG uptake rate of the control lung (0.00318 and 0.00315 min^{-1}) was virtually identical to that of the test lung (0.00337 min^{-1} for both animals).

Relation between [^{18}F]FDG Uptake and Neutrophil Count

Lung neutrophil count was significantly higher in the test lung of the NEEP group than in that of the PEEP group (1,046 ± 623 *vs.* 29 ± 59; $P < 0.05$), whereas it was similar in the control lung of the two groups (2 ± 3 and 2 ± 5). The difference in [^{18}F]FDG uptake rate between the test and control lungs was positively correlated (Pearson coefficient, 0.72; Spearman coefficient, 0.93; $P < 0.05$ for both) with the difference in neutrophil count (fig. 9).

To further ascertain the contribution of neutrophils to the [^{18}F]FDG signal in this VILI model, two additional sheep were submitted to the NEEP injury protocol after moderate or severe systemic neutrophil depletion. [^{18}F]FDG uptake of the test lung decreased markedly with decreasing *blood* neutrophil count, whereas the reduction of [^{18}F]FDG uptake was negligible in the control lung (fig. 10). Even in the sheep with severe neutrophil depletion, however, the [^{18}F]FDG uptake rate of the test lung remained higher than that of the control lung.

Observation of tissue sections revealed histopatho-

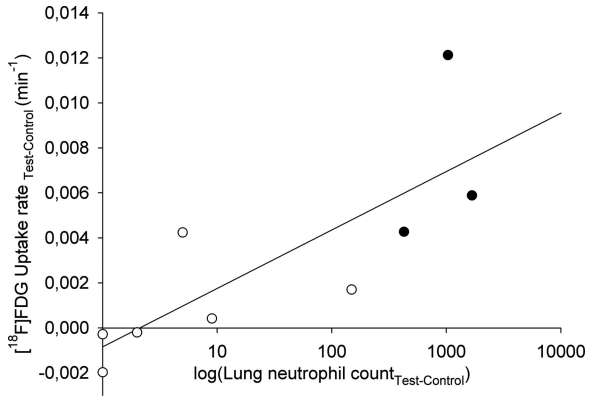

Fig. 9. Difference in [^{18}F]fluorodeoxyglucose ([^{18}F]FDG) uptake rate between the test and control lungs *versus* difference in lung neutrophil count, in semilogarithmic scale, in three animals of the negative end-expiratory pressure group (*filled symbols*) and in the six animals of the positive end-expiratory pressure group (*open symbols*). The semilogarithmic scale is used to represent the data in this figure because of the large disparity in neutrophil count of the test lung between the negative end-expiratory pressure and positive end-expiratory pressure groups. The correlation, however, was tested in linear, not in semilogarithmic, scale (Pearson coefficient, 0.72; Spearman coefficient, 0.93; $P < 0.05$ for both).

logic signs of VILI such as heterogeneous distension of alveoli, neutrophil infiltration, and intraalveolar proteinaceous material (light blue tinted with toluidine blue stain) in the test lung of the NEEP group, whereas alveoli were well distended with scant intraalveolar neutrophils in the test lung of the PEEP group (fig. 11).

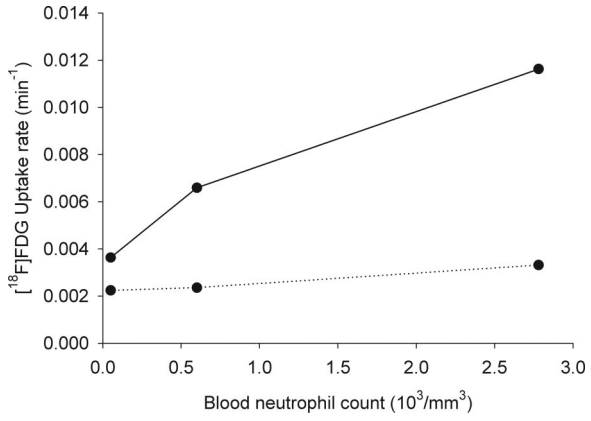

Fig. 10. [^{18}F]fluorodeoxyglucose ([^{18}F]FDG) uptake rate in test lungs (data points connected by *solid line*) and control lungs (data points connected by *dotted line*) *versus* circulating neutrophil count in the last animal of the negative end-expiratory pressure group (*rightmost pair* of data points, corresponding to the *filled hexagons* in fig. 8A) and in two animals submitted to the negative end-expiratory pressure injury protocol after either moderate or severe systemic neutrophil depletion. Note the progressive, marked reduction of [^{18}F]FDG uptake with decreasing blood neutrophils in the test lungs. Minimal reduction is observed in the control lungs. Note, however, that even with virtually complete neutrophil depletion (*leftmost pair* of data points), [^{18}F]FDG uptake rate remained higher in the test than in the control lung, suggesting that other cell types may have also been activated by injurious ventilation and contributed to the [^{18}F]FDG signal.

Discussion

The main findings of this study were as follows: (1) PET with [^{18}F]FDG and $^{13}N_2$ could quantify, noninvasively and *in vivo*, the regional pulmonary neutrophil activation and impairment of gas exchange caused by injurious mechanical ventilation; and (2) pulmonary metabolic activation could be detected within 90 min of dynamic overdistension without repetitive end-expiratory derecruitment, even though regional and global gas exchange and respiratory compliance were still preserved and histopathologic changes were not yet evident.

Interpretation of [^{18}F]FDG Uptake

Using microautoradiography of tissue sections after intravenous administration of [^{3}H]deoxyglucose, Jones *et al.*[17,18] demonstrated that deoxyglucose uptake by inflammatory cells is virtually confined to neutrophils during both acute and chronic lung inflammation. In this study, the contribution of neutrophils to the [^{18}F]FDG signal was confirmed by two observations. First, there was a positive correlation between [^{18}F]FDG uptake and lung neutrophil count. Second, [^{18}F]FDG uptake decreased markedly in the test lung with progressive systemic neutrophil depletion.

Because hyperinflation of the test lung of the PEEP group persisted after injury, we normalized the [^{18}F]FDG uptake rate to tissue fraction. Whereas the unnormalized rate depends both on density and metabolic activity of lung tissue,[19] the normalized rate should reflect only the mean *level* of cellular metabolic activity in the tissue compartment, after accounting for differences in lung inflation or in the volume of inflammatory infiltrate. Consequently, we used the normalized rate to measure the effect of injurious ventilation on the metabolic rate of a unit of tissue (*i.e.*, specific metabolic activity) and determine whether pure overdistension induced cell activation in the PEEP test lung, after accounting for the increased aeration of this lung.

Rationale of the Experimental Model

We used the suspended prone position to minimize baseline intraregional mechanical and functional heterogeneity[34] so that the source of mechanical lung stress would be largely under the control of external ventilatory pressure. The potential relevance of this approach lies in the argument that levels of mechanical stress comparable to those used in this study can develop regionally in the heterogeneously inflated acutely injured lung even when transpulmonary pressure is within narrower limits than those used in this study.[27]

Three observations argue against the possibility that the reduction in gas fraction with increase in shunt and the increase in [^{18}F]FDG uptake of the test lung of the NEEP group were due exclusively to transient atelectasis

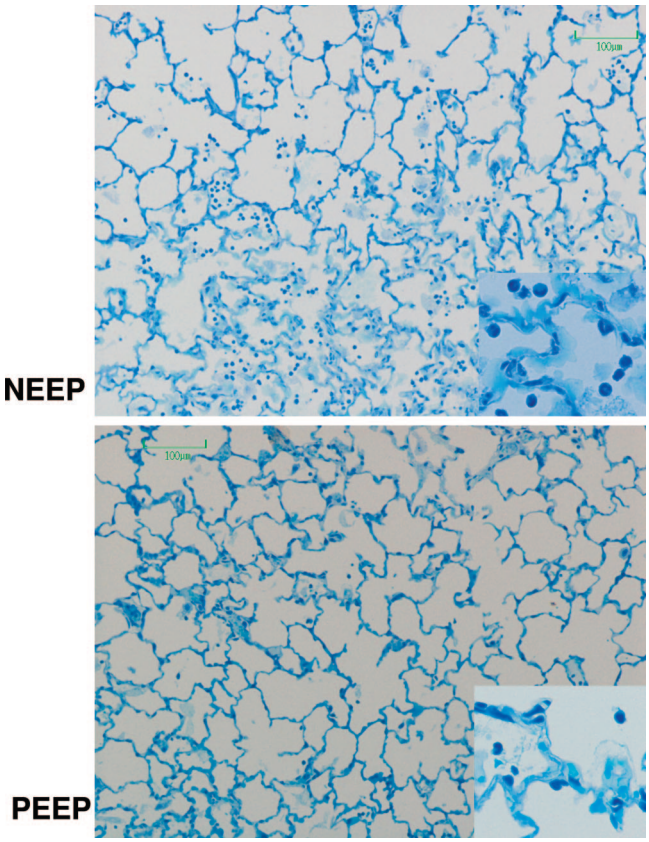

Fig. 11. Lung tissue sections of the test lung of one animal in the negative end-expiratory pressure (NEEP) group and one in the positive end-expiratory pressure (PEEP) group, stained with toluidine blue. The test lung of the NEEP group shows coexistence of poorly distended areas (*bottom of section*) with well distended and aerated areas (*top of section*), intraalveolar proteinaceous material, and marked cellular infiltration. At a fourfold higher magnification, intraalveolar cells seem to be mainly neutrophils (*inset*). The test lung of the PEEP group shows uniform alveolar distension and some neutrophils.

or negative pressure edema rather than to VILI. First, the recruitment maneuver performed after injury should have reversed transient atelectasis. Second, [^{18}F]FDG uptake remained higher in the test than in the control lung of the NEEP group even after normalization by tissue fraction. Because nonspecific leakage of [^{18}F]FDG into edema fluid does not significantly increase the [^{18}F]FDG uptake rate[21] whereas edema reduces gas fraction, edema in the absence of cell activation would be expected to lead to a reduction, not an increase, of normalized [^{18}F]FDG uptake rate compared with the nonedematous control lung, similarly to the normalization by the initial volume of distribution of [^{18}F]FDG.[51] Nor should atelectasis in the absence of cell activation increase the normalized [^{18}F]FDG uptake rate compared with the nonatelectatic control lung, because normalization by tissue fraction is expected to compensate for differences in lung inflation. Although use of 100% oxygen may have favored formation of resorption atelectasis,[52] it should have also minimized the injurious effect of atelectasis by attenuating hypoxia in atelectatic regions.[53] Consistent with the concept that NEEP *per se* did not result in increased [^{18}F]FDG uptake, there was no rise in [^{18}F]FDG uptake in the two lungs ventilated at NEEP without end-inspiratory overdistension. Third, histologic analysis revealed marked neutrophil infiltration and other signs of VILI in the test lung of the NEEP group. Furthermore, ventilation with repetitive end-expiratory derecruitment and recruitment has been shown to induce a cytokine response in the isolated lung.[54] These considerations do not imply absence of atelectasis or edema in our model, both of which are expected from impaired surfactant function and increased alveolocapillary permeability due to large tidal excursion[5,6,9,10,33,55] and repeated alveolar collapse and expansion,[30,37,56] but suggest that the functional, metabolic, and histologic changes observed were not due simply to transient atelectasis or edema but to VILI.

Effect of Injurious Ventilation on Regional Gas Exchange and Cellular Metabolic Activity

Neutrophils play a crucial role in the pathogenesis of VILI.[14,57,58] When overdistension was accompanied by repetitive end-expiratory derecruitment and recruitment, we could detect increased [^{18}F]FDG uptake, neutrophil infiltration, decreased aeration, and increased shunt fraction within 90 min of the start of injurious ventilation. This time interval is much shorter than that required to observe VILI in large,[2–4] as opposed to small,[5–7] animals exposed to overdistension without end-expiratory derecruitment. The mechanisms by which derecruitment may contribute to VILI include concentration of stress in the parenchyma around an atelectatic region[27] and dynamic shear stress on airway and alveolar epithelium when recruitment ensues.[59,60] Interestingly, cell activation occurred also after 90 min of overdistension without end-expiratory derecruitment, as shown by increased specific metabolic activity of the test lung in the PEEP group. In this lung, however, shunt fraction was not increased and neutrophil count was lower than in the NEEP group, in line with previous studies showing that 24–48 h was necessary to observe gas exchange impairment and histopathologic changes in response to overdistension alone in sheep.[2,3] Taken together, these findings suggest that a brief period of dynamic overdistension induced cell activation irrespective of the presence or absence of end-expiratory derecruitment, but concomitant repetitive derecruitment and recruitment, with larger tidal excursion, rapidly converted this activation into a profound inflammatory response with impairment in gas exchange.

The finding that a brief period of pure overdistension was sufficient to induce cell activation in a large animal with pulmonary physiology similar to the human and in the absence of other signs of VILI is potentially clinically relevant because regional overdistension could occur even at moderate transpulmonary pressure in a structur-

ally abnormal lung,[27] and hyperinflation, which can be associated with overdistension, has been shown in mechanically ventilated patients with ALI.[61] Overdistension, albeit of a lesser degree but possibly longer duration than in this study, could also occur in patients on single lung ventilation during thoracic surgery, if tidal volume is not reduced.[62]

An additional factor that could have delayed VILI in the test lung of the PEEP group was hypercapnia during the period of injury,[63–65] although pH, which is thought to mediate the protective effect of carbon dioxide in VILI,[66] was not significantly different between groups during injury.

The finding that specific metabolic activity was increased in the test lung of both groups can be reconciled with the significantly higher neutrophil count in the test lung of the NEEP group on two considerations. First, normalization of [^{18}F]FDG uptake rate by lung density is expected to account, at least in part, for the greater infiltration of activated neutrophils in the NEEP than in the PEEP test lung. Second, injurious ventilation could promote metabolic activation of other cell types such as vascular endothelial cells,[67] which are activated by tidal overdistension and can promote leukocyte recruitment,[68] and pneumocytes, which can act as a mechanosensor in response to cyclic stretch.[69] The fact that [^{18}F]FDG uptake remained higher in the test than in the control lung after virtually complete neutrophil depletion suggests that, even with neutrophils as the main contributors to the [^{18}F]FDG signal, other cells were activated by the injurious ventilation, similarly to what has been reported for endotoxin-induced ALI in mice.[70]

The finding that [^{18}F]FDG uptake of the control lung was remarkably similar between groups despite higher neutrophil count and unnormalized [^{18}F]FDG uptake of the test lung in the NEEP than in the PEEP group suggests that the neutrophilic inflammation induced in the test lung did not propagate systemically to the control lung. In addition, the fact that [^{18}F]FDG uptake of the control lung in the NEEP injury protocol was virtually independent of circulating neutrophil count (*i.e.*, the slope of the dotted line in fig. 10 is close to zero) would argue against the hypothesis that systemic neutrophil activation induced by localized VILI mediated significant inflammation of the contralateral lung. Remote inflammation in this VILI model, however, could occur in organs other than the lung, involve pathways not assessable by [^{18}F]FDG or require longer to manifest.

In the NEEP group, the increase in global shunt fraction underestimated the increase in regional shunt fraction attributable to localized injury. This underestimation was due to two factors. First, shunt fraction remained low in the control lung. Second, perfusion redistributed away from the test lung in five of the six animals. The importance of perfusion redistribution in modulating the impact of regional shunt fraction on global shunt fraction is apparent from the behavior of the two animals of the NEEP group with the highest shunt fraction in the test lung (fig. 6). After injury, the animal corresponding to the filled circle did not redistribute perfusion from the shunting lung to the control lung (fig. 7). Accordingly, this animal had a high global shunt fraction (0.29). In contrast, the animal corresponding to the filled triangle, which had a similarly elevated shunt fraction in the test lung, redistributed perfusion away from this lung, thus maintaining a low global shunt fraction (0.06). In both animals, global shunt fraction equaled the perfusion-weighted average of the shunt fractions calculated with $^{13}N_2$ for the test and control lungs. Therefore, despite similarly severe gas exchange impairment in the injured lung, in one of these animals global shunt fraction markedly underestimated the severity of regional dysfunction because of perfusion redistribution away from the shunting lung, possibly due to strong hypoxic pulmonary vasoconstriction. This case exemplifies the potential limitation of relying on global shunt fraction, and for that matter Pa_{O_2}, to infer the severity of a pulmonary process that is spatially heterogeneous, like ALI. When the loss of aeration is heterogeneous, perfusion redistribution from poorly aerated shunting regions to well-aerated regions will affect the degree of hypoxemia.[36,71]

In summary, PET can measure the pulmonary metabolic activation of neutrophils during VILI. This technique had sufficient sensitivity to show that activation occurred in response to a brief period of pure overdistension, even in the absence of deterioration in regional or global gas exchange. Concomitant repetitive derecruitment and recruitment, with larger tidal excursion, rapidly converted this activation into a profound localized inflammatory cell response with regional impairment of gas exchange.

The authors thank Steven B. Weise (Senior Research Technician, Division of Nuclear Medicine, Massachusetts General Hospital, Boston, Massachusetts) and Sandra A. Barrow (Certified Nuclear Medicine Technician, Division of Nuclear Medicine, Massachusetts General Hospital) for image acquisition and processing; Peter A. Rice, B.S., R.Ph., and Stephen C. Dragotakes, R.Ph. (Certified Nuclear Pharmacists, Department of Radiology, Massachusetts General Hospital), John A. Correia, Ph.D. (Associate Professor of Radiology, Harvard Medical School, Boston, Massachusetts), William M. Buceliewicz and David F. Lee, B.S. (Senior Cyclotron Engineers, Department of Radiology, Massachusetts General Hospital), for preparation of the radioisotopes; Olga Syrkina, M.D. (Pulmonary and Critical Care Unit, Department of Medicine, Massachusetts General Hospital), for animal preparation; and Rosemary C. Jones, Ph.D. (Associate Professor of Pathology, Harvard Medical School), and Diane E. Capen, B.A. (Senior Research Technician, Department of Anesthesia and Critical Care, Massachusetts General Hospital), for assistance with histologic analysis.

References

1. The Acute Respiratory Distress Syndrome Network: Ventilation with lower tidal volumes as compared with traditional tidal volumes for acute lung injury and the acute respiratory distress syndrome. N Engl J Med 2000; 342:1301–8

2. Kolobow T, Moretti MP, Fumagalli R, Mascheroni D, Prato P, Chen V, Joris M: Severe impairment in lung function induced by high peak airway pressure during mechanical ventilation: An experimental study. Am Rev Respir Dis 1987; 135:312–5

3. Tsuno K, Prato P, Kolobow T: Acute lung injury from mechanical ventilation at moderately high airway pressures. J Appl Physiol 1990; 69:956–61

4. Tsuno K, Miura K, Takeya M, Kolobow T, Morioka T: Histopathologic pulmonary changes from mechanical ventilation at high peak airway pressures. Am Rev Respir Dis 1991; 143:1115–20

5. Dreyfuss D, Basset G, Soler P, Saumon G: Intermittent positive-pressure hyperventilation with high inflation pressures produces pulmonary microvascular injury in rats. Am Rev Respir Dis 1985; 132:880–4

6. Dreyfuss D, Soler P, Basset G, Saumon G: High inflation pressure pulmonary edema: Respective effects of high airway pressure, high tidal volume, and positive end-expiratory pressure. Am Rev Respir Dis 1988; 137:1159–64

7. Dreyfuss D, Saumon G: Role of tidal volume, FRC, and end-inspiratory volume in the development of pulmonary edema following mechanical ventilation. Am Rev Respir Dis 1993; 148:1194–203

8. Muscedere JG, Mullen JBM, Gan K, Slutsky AS: Tidal ventilation at low airway pressures can augment lung injury. Am J Respir Crit Care Med 1994; 149:1327–34

9. Webb HH, Tierney DF: Experimental pulmonary edema due to intermittent positive pressure ventilation with high inflation pressures: Protection by positive end-expiratory pressure. Am Rev Respir Dis 1974; 110:556–65

10. Hernandez LA, Peevy KJ, Moise AA, Parker JC: Chest wall restriction limits high airway pressure-induced lung injury in young rabbits. J Appl Physiol 1989; 66:2364–8

11. Zhang H, Downey GP, Suter PM, Slutsky AS, Ranieri VM: Conventional mechanical ventilation is associated with bronchoalveolar lavage-induced activation of polymorphonuclear leukocytes. ANESTHESIOLOGY 2002; 97:1426–33

12. Matsuoka T, Kawano T, Miyasaka K: Role of high-frequency ventilation in surfactant-depleted lung injury as measured by granulocytes. J Appl Physiol 1994; 76:539–44

13. Sugiura M, McCulloch PR, Wren S, Dawson RH, Froese AB: Ventilator pattern influences neutrophil influx and activation in atelectasis-prone rabbit lung. J Appl Physiol 1994; 77:1355–65

14. Kawano T, Mori S, Cybulsky M, Burger R, Ballin A, Cutz E, Bryan AC: Effect of granulocyte depletion in a ventilated surfactant-depleted lung. J Appl Physiol 1987; 62:27–33

15. Karzai W, Cui X, Heinicke N, Niemann C, Gerstenberger EP, Correa R, Banks S, Mehlhorn B, Bloos F, Reinhart K, Eichacker PQ: Neutrophil stimulation with granulocyte colony-stimulating factor worsens ventilator-induced lung injury and mortality in rats. ANESTHESIOLOGY 2005; 103:996–1005

16. Martin TR: Neutrophils and lung injury: Getting it right. J Clin Invest 2002; 110:1603–5

17. Jones HA, Clark RJ, Rhodes CG, Schofield JB, Krausz T, Haslett C: *In vivo* measurement of neutrophil activity in experimental lung inflammation. Am J Respir Crit Care Med 1994; 149:1635–9

18. Jones HA, Schofield JB, Krausz T, Boobis AR, Haslett C: Pulmonary fibrosis correlates with duration of tissue neutrophil activation. Am J Respir Crit Care Med 1998; 158:620–8

19. Jones HA, Sriskandan S, Peters AM, Pride NB, Krausz T, Boobis AR, Haslett C: Dissociation of neutrophil emigration and metabolic activity in lobar pneumonia and bronchiectasis. Eur Respir J 1997; 10:795–803

20. Jones HA, Cadwallader KA, White JF, Uddin M, Peters AM, Chilvers ER: Dissociation between respiratory burst activity and deoxyglucose uptake in human neutrophil granulocytes: Implications for interpretation of ^{18}F-FDG PET images. J Nucl Med 2002; 43:652–7

21. Chen DL, Schuster DP: Positron emission tomography with [^{18}F]fluorodeoxyglucose to evaluate neutrophil kinetics during acute lung injury. Am J Physiol Lung Cell Mol Physiol 2004; 286:L834–40

22. Kirpalani H, Abubakar K, Nahmias C, deSa D, Coates G, Schmidt B: [^{18}F]Fluorodeoxyglucose uptake in neonatal acute lung injury measured by positron emission tomography. Pediatr Res 1997; 41:892–6

23. Jones HA, Marino PS, Shakur BH, Morrell NW: *In vivo* assessment of lung inflammatory cell activity in patients with COPD and asthma. Eur Respir J 2003; 21:567–73

24. Monkman SL, Andersen CC, Nahmias C, Ghaffer H, Bourgeois JM, Roberts RS, Schmidt B, Kirpalani HM: Positive end-expiratory pressure above lower inflection point minimizes influx of activated neutrophils into lung. Crit Care Med 2004; 32:2471–5

25. Farre R, Granell S, Rotger M, Serrano-Mollar A, Closa D, Navajas D: Animal model of unilateral ventilator-induced lung injury. Intensive Care Med 2005; 31:487–90

26. Valenza F, Guglielmi M, Irace M, Porro GA, Sibilla S, Gattinoni L: Positive end-expiratory pressure delays the progression of lung injury during ventilator strategies involving high airway pressure and lung overdistension. Crit Care Med 2003; 31:1993–8

27. Mead J, Takishima T, Leith D: Stress distribution in lungs: A model of pulmonary elasticity. J Appl Physiol 1970; 28:596–608

28. Bregeon F, Delpierre S, Chetaille B, Kajikawa O, Martin TR, Autillo-Touati A, Jammes Y, Pugin J: Mechanical ventilation affects lung function and cytokine production in an experimental model of endotoxemia. ANESTHESIOLOGY 2005; 102:331–9

29. Schreiber T, Hueter L, Schwarzkopf K, Hohlstein S, Schmidt B, Karzai W: Increased susceptibility to ventilator-associated lung injury persists after clinical recovery from experimental endotoxemia. ANESTHESIOLOGY 2006; 104:133–41

30. Taskar V, John J, Evander E, Robertson B, Jonson B: Surfactant dysfunction makes lungs vulnerable to repetitive collapse and reexpansion. Am J Respir Crit Care Med 1997; 155:313–20

31. Nahum A, Hoyt J, Schmitz L, Moody J, Shapiro R, Marini JJ: Effect of mechanical ventilation strategy on dissemination of intratracheally instilled *Escherichia coli* in dogs. Crit Care Med 1997; 25:1733–43

32. Ye SQ, Simon BA, Maloney JP, Zambelli-Weiner A, Gao L, Grant A, Easley RB, McVerry BJ, Tuder RM, Standiford T, Brower RG, Barnes KC, Garcia JGN: Pre-B-cell colony-enhancing factor as a potential novel biomarker in acute lung injury. Am J Respir Crit Care Med 2005; 171:361–70

33. Greenfield LJ, Ebert PA, Benson DW: Effect of positive pressure ventilation on surface tension properties of lung extracts. ANESTHESIOLOGY 1964; 25:312–6

34. Richter T, Bellani G, Harris RS, Vidal Melo MF, Winkler T, Venegas JG, Musch G: Effect of prone position on regional shunt, aeration and perfusion in experimental acute lung injury. Am J Respir Crit Care Med 2005; 172:480–7

35. Vidal Melo MF, Harris RS, Layfield D, Musch G, Venegas JG: Changes in regional ventilation after autologous blood clot pulmonary embolism. ANESTHESIOLOGY 2002; 97:671–81

36. Musch G, Harris RS, Vidal Melo MF, O'Neill KR, Layfield JDH, Winkler T, Venegas JG: Mechanism by which a sustained inflation can worsen oxygenation in acute lung injury. ANESTHESIOLOGY 2004; 100:323–30

37. Taskar V, John J, Evander E, Wollmer P, Robertson B, Jonson B: Healthy lungs tolerate repetitive collapse and reopening during short periods of mechanical ventilation. Acta Anaesthesiol Scand 1995; 39:370–6

38. Laffey JG, Engelberts D, Kavanagh BP: Injurious effects of hypocapnic alkalosis in the isolated lung. Am J Respir Crit Care Med 2000; 162:399–405

39. Sharan M, Popel AS: Algorithm for computing oxygen dissociation curve with pH, PCO_2, and CO in sheep blood. J Biomed Eng 1989; 11:48–52

40. Warner MA, Divertie MB, Offord KP, Marsh HM, Helmholz HF, McMichan JC: Clinical implications of variation in total venoarterial shunt fraction calculated by different methods during severe acute respiratory failure. Mayo Clin Proc 1983; 58:654–9

41. Musch G, Foti G, Cereda M, Pelosi P, Poppi D, Pesenti A: Lung and chest wall mechanics in normal anaesthetized subjects and in patients with COPD at different PEEP levels. Eur Respir J 1997; 10:2545–52

42. Vidal Melo MF, Layfield D, Harris RS, O'Neill K, Musch G, Richter T, Winkler T, Fischman AJ, Venegas JG: Quantification of regional ventilation-perfusion ratios with PET. J Nucl Med 2003; 44:1982–91

43. Musch G, Layfield JDH, Harris RS, Vidal Melo MF, Winkler T, Callahan RJ, Fischman AJ, Venegas JG: Topographical distribution of pulmonary perfusion and ventilation, assessed by PET in supine and prone humans. J Appl Physiol 2002; 93:1841–51

44. Harris RS, Willey-Courand DB, Head CA, Galletti GG, Call DM, Venegas JG: Regional V_A, Q, and V_A/Q during PLV: Effects of nitroprusside and inhaled nitric oxide. J Appl Physiol 2002; 92:297–312

45. Mijailovich SM, Treppo S, Venegas JG: Effects of lung motion and tracer kinetics corrections on PET imaging of pulmonary function. J Appl Physiol 1997; 82:1154–62

46. Galletti GG, Venegas JG: Tracer kinetic model of regional pulmonary function using positron emission tomography. J Appl Physiol 2002; 93:1104–14

47. O'Neill K, Venegas JG, Richter T, Harris RS, Layfield JDH, Musch G, Winkler T, Vidal Melo MF: Modeling kinetics of infused ^{13}NN-saline in acute lung injury. J Appl Physiol 2003; 95:2471–84

48. Patlak CS, Blasberg RG, Fenstermacher JD: Graphical evaluation of blood-to-brain transfer constants from multiple-time uptake data. J Cereb Blood Flow Metab 1983; 3:1–7

49. Patlak CS, Blasberg RG: Graphical evaluation of blood-to-brain transfer constants from multiple-time uptake data: Generalizations. J Cereb Blood Flow Metab 1985; 5:584–90

50. Beppu H, Ichinose F, Kawai N, Jones RC, Yu PB, Zapol WM, Miyazono K, Li E, Bloch KD: BMPR-II heterozygous mice have mild pulmonary hypertension and an impaired pulmonary vascular remodeling response to prolonged hypoxia. Am J Physiol Lung Cell Mol Physiol 2004; 287:L1241–7

51. Chen DL, Mintun MA, Schuster DP: Comparison of methods to quantitate ^{18}F-FDG uptake with PET during experimental acute lung injury. J Nucl Med 2004; 45:1583–90

52. Duggan M, Kavanagh BP: Pulmonary atelectasis: A pathogenic perioperative entity. ANESTHESIOLOGY 2005; 102:838–54

53. Duggan M, McNamara PJ, Engelberts D, Pace-Asciak C, Babyn P, Post M, Kavanagh BP: Oxygen attenuates atelectasis-induced injury in the *in vivo* rat lung. ANESTHESIOLOGY 2005; 103:522–31

54. Cheng KC, Zhang H, Lin CY, Slutsky AS: Ventilation with negative airway pressure induces a cytokine response in isolated mouse lung. Anesth Analg 2002; 94:1577–82

55. Faridy EE, Permutt S, Riley RL: Effect of ventilation on surface forces in excised dogs' lungs. J Appl Physiol 1966; 21:1453–62

56. Faridy EE: Effect of ventilation on movement of surfactant in airways. Respir Physiol 1976; 27:323–34

57. Belperio JA, Keane MP, Burdick MD, Londhe V, Xue YY, Li K, Phillips RJ, Strieter RM: Critical role for CXCR2 and CXCR2 ligands during the pathogenesis of ventilator-induced lung injury. J Clin Invest 2002; 110:1703–16

58. Caironi P, Ichinose F, Liu R, Jones RC, Bloch KD, Zapol WM: 5-Lipoxy-

genase deficiency prevents respiratory failure during ventilator-induced lung injury. Am J Respir Crit Care Med 2005; 172:334–43

59. Nucci G, Suki B, Lutchen K: Modeling airflow-related shear stress during heterogeneous constriction and mechanical ventilation. J Appl Physiol 2003; 95:348–56

60. Bilek AM, Dee KC, Gaver DP: Mechanisms of surface-tension-induced epithelial cell damage in a model of pulmonary airway reopening. J Appl Physiol 2003; 94:770–83

61. Nieszkowska A, Lu Q, Vieira S, Elman M, Fetita C, Rouby JJ: Incidence and regional distribution of lung overinflation during mechanical ventilation with positive end-expiratory pressure. Crit Care Med 2004; 32:1496–503

62. Fernandez-Perez ER, Keegan MT, Brown DR, Hubmayr RD, Gajic O: Intraoperative tidal volume as a risk factor for respiratory failure after pneumonectomy. ANESTHESIOLOGY 2006; 105:14–8

63. Broccard AF, Hotchkiss JR, Vannay C, Markert M, Sauty A, Feihl F, Schaller MD: Protective effects of hypercapnic acidosis on ventilator-induced lung injury. Am J Respir Crit Care Med 2001; 164:802–6

64. Sinclair SE, Kregenow DA, Lamm WJE, Starr IR, Chi EY, Hlastala MP: Hypercapnic acidosis is protective in an *in vivo* model of ventilator-induced lung injury. Am J Respir Crit Care Med 2002; 166:403–8

65. Laffey JG, Engelberts D, Duggan M, Veldhuizen R, Lewis JF, Kavanagh BP: Carbon dioxide attenuates pulmonary impairment resulting from hyperventilation. Crit Care Med 2003; 31:2634–40

66. Laffey JG, O'Croinin D, McLoughlin P, Kavanagh BP: Permissive hypercapnia: Role in protective lung ventilatory strategies. Intensive Care Med 2004; 30:347–56

67. Maschauer S, Prante O, Hoffmann M, Deichen JT, Kuwert T: Characterization of ^{18}F-FDG uptake in human endothelial cells *in vitro*. J Nucl Med 2004; 45:455–60

68. Yiming MT, Parthasarathi K, Issekutz AC, Bhattacharya S: Sequence of endothelial signaling during lung expansion. Am J Respir Cell Mol Biol 2005; 33:549–54

69. Vlahakis NE, Schroeder MA, Limper AH, Hubmayr RD: Stretch induces cytokine release by alveolar epithelial cells *in vitro*. Am J Physiol (Lung Cell Mol Physiol) 1999; 277:L167–73

70. Zhou Z, Kozlowski J, Goodrich AL, Markman N, Chen DL, Schuster DP: Molecular imaging of lung glucose uptake after endotoxin in mice. Am J Physiol Lung Cell Mol Physiol 2005; 289:L760–8

71. Easley RB, Fuld MK, Fernandez-Bustamante A, Hoffman EA, Simon BA: Mechanism of hypoxemia in acute lung injury evaluated by multidetector-row CT. Acad Radiol 2006; 13:916–21